1 **Dual thermal ecotypes detected within a nearly genetically-identical population of the**

2 **unicellular marine cyanobacterium *Synechococcus***

3

4 Joshua D. Kling[1], Michael D. Lee[2,3], Eric A. Webb[1], Jordan T. Coelho[1], Paul Wilburn[2,4],

5 Stephanie I. Anderson[5], Qianqian Zhou[6], Chunguang Wang[6], Megan D. Phan[1], Feixue Fu[1], Colin

6 T. Kremer[4], Elena Litchman[4], Tatiana A. Rynearson[5], David A. Hutchins[1]

7

8 *[1]Department of Biological Sciences, University of Southern California, Los Angeles, CA 90007, USA*

9 *[2]Exobiology Branch, NASA Ames Research Center, Mountain View, CA 94035, USA*

10 *[3]Blue Marble Space Institute of Science, Seattle, WA 98154, USA*

11 *[4]Kellogg Biological Station, Michigan State University, Hickory Corners, MI 49060, USA*

12 *[5]Graduate School of Oceanography, The University of Rhode Island, Kingston, RI 02881, USA*

13 *[6]Third Institute of Oceanography, Ministry of Natural Resources, Xiamen, 361005, Fujian, China*

14 ***Corresponding Author:**

15 David A. Hutchins

16 Address: 3616 Trousdale Parkway, AHF 207, Los Angeles, CA 90007

17 Email: dahutch@usc.edu

18

19 **Keywords:** *Synechococcus* | temperature adaptation | Intraspecific diversity | phycocyanin

20 **Author Contributions:**

21 Isolates were collected by JDK, PW, SIA, EL, TAR, & DAH, and subsequent culture work and

22 its analysis done by JDK, MDP, EAW, FU, CTK. DNA extraction, sequencing, and analysis

23 performed by JDK, MDL, JTC, QZ, & CW. All authors contributed to the writing.

24 **Significance**

25 Numerous studies exist comparing the responses of distinct taxonomic groups of marine

26 microbes to a warming ocean (interspecific thermal diversity). For example, *Synechococcus,* a

27 nearly globally distributed unicellular marine picocyanobacterium that makes significant

28 contributions to oceanic primary productivity, contains numerous taxonomically distinct lineages

29 with well documented temperature relationships. Little is known though about the diversity of

30 functional responses to temperature within a given population where genetic similarity is high

31 (intraspecific thermal diversity). This study suggests that understanding the extent of this

32 functional intraspecific microdiversity is an essential prerequisite to predicting the resilience of

33 biogeochemically essential microbial groups such as marine *Synechococcus* to a changing

34 climate.

35

36   **Abstract**

37   The extent and ecological significance of intraspecific diversity within marine microbial

38   populations is still poorly understood, and it remains unclear if such strain-level microdiversity

39   will affect fitness and persistence in a rapidly changing ocean environment. In this study, we

40   cultured 11 sympatric strains of the ubiquitous marine picocyanobacterium *Synechococcus*

41   isolated from a Narragansett Bay (Rhode Island, USA) phytoplankton community thermal

42   selection experiment. Despite all 11 isolates being highly similar (with average nucleotide

43   identities of >99.9%, with 98.6-100% of the genome aligning), thermal performance curves

44   revealed selection at warm and cool temperatures had subdivided the initial population into

45   thermotypes with pronounced differences in maximum growth temperatures. Within the fine-

46   scale genetic diversity that did exist within this population, the two divergent thermal ecotypes

47   differed at a locus containing genes for the phycobilisome antenna complex. Our study

48   demonstrates that present-day marine microbial populations can contain microdiversity in the

49   form of cryptic but environmentally-relevant thermotypes that may increase their resilience to

50   future rising temperatures.

Introduction

Marine bacteria control most marine biogeochemical cycles (1, 2) and are composed of an estimated 10^{10} species (3). In addition, bacterial species complexes also include numerous strains or ecotypes (4–8). Much of the work documenting the ecological relevance of intraspecific microdiversity has used amplified marker genes such as the 16S rRNA gene, resolved to single base pair differences (9). However, there is still much work to be done to describe the potentially substantial genotypic and (more importantly) phenotypic diversity that exists within groups that are highly similar or even identical at the 16S rRNA level. At higher taxonomic levels, microbial interspecific diversity has a recognized role increasing the stability of biogeochemical cycling and resilience to a changing environment (10). In order to understand the ability of microbial populations to persist and maintain their functional roles under changing thermal regimes, however, it is also important to understand how much unrecognized microdiversity relevant to future warmer temperatures currently exists within microbial populations (11–13).

Efforts to understand the interactions of microbes with the marine environment have often relied on approaches that underestimate or mask intraspecific diversity. For instance, culture-based methods are often limited to a handful of strains that are amenable to cultivation or are currently available in culture collections. These are then used to make generalizations about the activity of a broader taxonomic group (14–16). Sequencing approaches avoid this culturing bottleneck but lack the ability to provide rate measurements. Furthermore, metagenomic or metatranscriptomic analysis pipelines often are unable to discern sequencing errors from rare genotypes or strains (17). In addition, purely sequence-based *in situ* approaches are also limited in the amount of ecotype microdiversity they can reveal, simply because detection relies on

4

74 observed correlations between relative abundance and ambient environmental parameters (e.g.

75 temperature, nutrients, light). Thus, rare ecotypes with optimal niches that lie outside of current

76 conditions will remain cryptic unless the environment changes. For example, most marine

77 microbial communities will undergo future selection by temperatures exceeding those that they

78 currently experience (18, 19), as current climate models predict that anthropogenic carbon

79 emissions will raise sea surface temperatures ~4°C by the year 2100 (20).

80   Marine unicellular picocyanobacteria are particularly important to our understanding of

81 how microbially mediated biogeochemical cycling will change with rising sea surface

82 temperatures (SST). The unicellular marine cyanobacterium *Synechococcus* is a major microbial

83 functional and taxonomic group that is found from the equator to high polar latitudes (8, 21).

84 This widespread and diverse genus is responsible for an estimated 16.7% of marine primary

85 production, and is expected to increase in both abundance and distribution as result of climate

86 warming (22). It has also been strongly correlated with carbon export to the deep ocean (23),

87 making this genus an important component of the marine carbon cycle.

88   In this study, we used multiple temperature incubations of a natural coastal assemblage to

89 enrich for 'thermal specialist' strains of *Synechococcus*. We then isolated multiple sympatric

90 strains from the contrasting temperature incubations and characterized their thermal niches,

91 allowing us to recover two co-occuring but distinct thermal phenotypes from a single initial

92 water sample. Finally, we used high-coverage, short read sequencing to obtain high-quality draft

93 genomes for all of the isolates. Upon comparing their assemblies, the two sets of thermally-

94 distinct isolates are nearly identical, with an average nucleotide identity (ANI) > 99.9%

95 demonstrating that these thermotypes belong to the same population. We additionally detected

96 genetic variation that differentiates both thermotypes in a locus coding for the photosynthetic

97   accessory pigment C-phycocyanin. This trait's relevance is not immediately apparent within the

98   current study's context, but is nevertheless strongly correlated with the identifiable thermal

99   specializations observed in this population.

100   **Results**

101   Out of the 11 strains of *Synechococcus* isolated in this study, one originated from our

102   initial cell sorting of the collected seawater (at 22°C), before nutrients were added (Table S1).

103   The other ten isolates were collected from the enrichment experiments, five from an 18 °C

104   enrichments and five from 30 °C. Because the 22°C *in situ* conditions and 18°C experimental

105   treatment represent temperatures that currently occur in Narragansett Bay, these isolates are

106   considered together and are referred to as "cool temperature isolates" and compared against

107   "warm temperature isolates" collected from 30 °C (a temperature exceeding those currently

108   recorded at this sampling site). Despite these considerable differences in temperature, all of the

109   cool and warm temperature isolates shared virtually identical morphologies (Table S1).

110   Picocyanobacteria were also detected in 22 and 26 °C temperature incubation treatments, but cell

111   sorting did not produce any culturable isolates from these incubations.

112   After growing each of the 11 isolates across multiple temperatures, we generated thermal

113   performance curves for each isolate, with an average R^2 of 0.81 (±0.14 SD, Figure 1A & S1;

114   Table S2). The average thermal maximum (Tmax) was highest for warm temperature isolates

115   (35.6 °C, ±0.5 SD) compared to cool temperature isolates (33.5 °C, ±0.9; t-test, $p = 0.005$; Figure

116   1B; Table 1). The optimal growth temperature (Topt) was also higher for isolates from warm

117   temperatures, with a mean of 29.8° (±1.8 SD), than for cool temperature (27.6 °C, ±1.2 SD);

118   however, this difference was not statistically significant ($p = 0.06$). Minimum growth

119   temperature (Tmin) and niche width (Tmax – Tmin) did not significantly differ between the two

6

120   groups ($p = 0.91$). In addition to differences in growth observed using *in vivo* fluorescence

121   measurements, we compared one warm and one cool temperature isolate (LA127 and LA31

122   respectively) when temperature was increased from 22 to 28 °C, closer to their Topt (Table S2).

123   This showed that the warm-temperature isolate accumulated ~2x more volume-normalized

124   particulate organic carbon (POC; $p = 0.002$; Figure S2A) and maintained a higher, but not

125   statistically significant ($p = 0.07$), growth rate (Figure S2B).

126   To compare genomic differences between cool and warm temperature isolates, sequence

127   data for each isolate collected from this study (n=11) was assembled and manually curated

128   producing estimated 100% complete draft genomes (Table S3). Recovered short read genomes

129   (hereafter called draft assemblies) were 2.74 Mbp long (±0.01 SD), split between an average of

130   22.1 (±6 SD) contigs with a mean GC content of 63.3% (±0.00) and mean gene count of 2976.0

131   (±11 SD) for each isolate. We generated long reads for one cool (LA31) and one warm

132   temperature isolate (LA127) and were able to close the genome of the warm temperature isolate

133   (one contig 2.75 Mbp long compared to 27 contigs from the short-read only assembly). Including

134   long reads substantially improved the assembly of the cool temperature isolate, reducing the

135   number of contigs from 18 to six (Table S3).

136   When constructing a phylogenetic tree with all presently available *Synechococcus*

137   genomes (Figure S2), the isolates from this study fell within the same clade as marine subcluster

138   5.2. With the level of resolution provided by 239 concatenated amino acid sequences, all 11 were

139   nearly indistinguishable from each other (Figure 2A). Interestingly, the most closely related

140   isolate in Genbank was CB0101 from Chesapeake Bay, another large coastal estuary located on

141   the east coast of the United States (24). High genetic relatedness was even more apparent using

142   average nucleotide identity (ANI), with greater than 99.99% (±0.003 SD) across 98.6-100% of

7

143   the assembly for all genomes (Figure 2B). For comparison, the average ANI between isolates

144   from this study and CB0101 was 85.46%.

145   Despite the high degree of similarity, when comparing draft assemblies from a

146   pangenomic perspective, 62 out of 2985 gene clusters were identified by Anvi'o (Figure S4,

147   Table S4) as having less than 100% functional (e.g. differences in sequence) or structural (e.g.

148   insertions, deletions) homogeneity between one or more assemblies. Manually examining these

149   gene clusters for genomic differences that correlated with isolation temperatures and measured

150   thermal performance curves revealed that many of the features causing this detected variation

151   were typically found only in one or a few isolates (Figure S5).

152   Only two gene clusters examined had patterns of variation that correlated with the

153   temperature treatments that these strains were isolated from (e.g. exclusive to warm temperature

154   isolates). These two gene clusters contain genes coding for the α and β subunits of the

155   photosynthetic accessory pigment C-phycocyanin (*cpcA* and *cpcB* respectively). Cool

156   temperature assemblies contained a complete copy of *cpcA*, while warm temperature assemblies

157   lacked a complete copy of the α phycocyanin subunit (Figure S6A). On the other hand, all but

158   one warm temperature isolate (LA126) had a complete copy of *cpcB,* while assemblies from cool

159   temperature isolates only had the first 25 and the last 56 amino acids from *cpcB* coded for on

160   different contigs (Figure S6B).

161   Because these differences in assembly between cool and warm temperature isolates are

162   for genes coding for accessory pigments, we compared photosystem function between

163   phenotypically distinct warm and cool temperature isolates. We measured whole-cell

164   fluorescence spectra matching C-phycocyanin across rising temperatures for cool temperature

165   strain LA31 (Topt = 27.5 °C, Tmax = 31.7 °C) and warm temperature strain LA127 (Topt = 29.7

166   °C, Tmax = 35.3 °C), using increasing fluorescence from initial levels at 22 °C as an indicator of

167   loss of photosynthetic function to heat stress. The warm temperature isolate had a lower change

168   in fluorescence at physiologically-relevant temperatures below 45 °C (Figure 3A). Fluorescence

169   for both isolates increased exponentially between 48-54 °C, before abruptly crashing to zero at

170   57 °C. This suggests that light-harvesting energetic losses to fluorescence increase as the

171   photosynthetic antenna complex becomes stressed by warming temperatures, before completely

172   disassociating at a critical high temperature and losing all fluorescence. The warm temperature

173   isolate had lower fluorescence at the fluorescence peak 54 °C (t-test, $p = 0.07$), suggesting it is

174   better able to maintain its functionality under extreme thermal stress (Figure 3A). Furthermore,

175   both isolates had differing photophysiologies when comparing the photosynthetic efficiency

176   parameter Fv/Fm (Figure 3B). When acclimated to 28° C the warm temperature isolate had

177   significantly higher values (t-test, $p = 1.04 \times 10^{-7}$), suggesting its photosystem II had a greater

178   photochemical efficiency than the cool temperature isolate. The values reported here are

179   analogous to Fv/Fm measurements reported for other marine *Synechococcus* spp. (25).

180   A closer look at the genes associated with C-phycocyanin was unable to discern the exact

181   genetic mechanism causing these measured differences in photosynthetic function. We compared

182   the closed warm temperature isolate genome (LA127) and the closed genome of the closely

183   related Chesapeake Bay strain CB0101, which revealed the majority of C-phycocyanin and

184   surrounding genes in the same orientation (Figure 4A). In all draft assemblies (short-read data

185   only), assembly failed at this exact locus (Figure 4B & C). Interestingly however, the pattern of

186   contig breakage is conserved for all draft assemblies of isolates from cool temperatures (breaking

187   within copies of *cpcB*, Figure 4B), while a distinct pattern of contig breaks is found in assemblies

188   of warm temperature isolates (breaking sooner in all cases, Figure 4C). These conserved contig-

189   breakage patterns within our cool and warm groups correlate with their measured differences in

190   thermal performance curves and photophysiology, suggesting whatever variation is consistently

191   leading to these assembly results may be involved in these phenotypic traits. Long-read

192   sequencing and assembly of all isolates may help further interrogate this region. For the two we

193   were able to attempt, although we spanned this difficult-to-assemble region for the warm

194   temperature isolate LA127, we were not able to for the cool temperature isolate LA31 (Figure

195   4D), preventing a direct comparison.

196   Mapping Illumina short-reads from all isolates to single complete copies of *cpcA* and

197   *cpcB* from draft assemblies showed some single nucleotide variants (SNVs; Supplemental Note 1

198   and Figure S7); however, no SNVs were detected when mapping short-reads to this locus on the

199   closed genome from LA127 (Supplemental Note 1 and Figure S8). This suggests that although

200   minor sequence differences were detected between the complete copies of these genes recovered

201   in the closed hybrid genome (Table S5 & S6), they were identical to the completely assembled

202   copies in the draft assemblies (Table S7). Mapping rates were used to attempt to detect different

203   gene copy numbers at this locus which might contribute to this systematic pattern contig

204   breakage (Supplemental Note 2); however, these data were inconclusive. Copy numbers of *cpcA*

205   and *cpcB* vary across Subcluster 5.2 genomes (Table S8) and these isolates appear to have

206   multiple copies of the genes (Figures S7-S10; Supplemental Note 2); however, we were not able

207   to deduce from these data whether or not copy number differed between isolates from different

208   temperatures. Although the exact genomic differences causing these assembly results are as yet

209   unclear, these contig breaks occur systematically between cool and warm temperature isolates.

210   As this correlates with the observed temperature responses (Figure 1), it suggests that genes

211   associated with accessory pigment C-phycocyanin production could be involved in thermal

212   adaptation.

Discussion

214   This study demonstrates the coexistence of distinct thermal phenotypes within a highly

215   genetically similar, single population of coastal cyanobacteria. The division of this estuarine

216   *Synechococcus* population into contrasting cool and warm thermotypes was revealed following

217   incubation experiments at 18 °C and 30 °C, in which strain-sorting was identified by culture

218   isolations and thermal phenotype determinations in the laboratory. By using high-coverage short

219   reads as well as long reads to reconstruct these isolates' genomes, we found that this striking

220   phenotypic divergence between thermotypes appears to be tied to very minor genetic differences.

221   Although previous work has established that distinct functionally-relevant ecotypes coexist

222   within populations of picocyanobacteria (e.g. Kashtan et al., 2014; Thompson & Kouba, 2019),

223   this is the first study to report coexisting ecotypes at this high level of genomic resolution.

224   Variation in assembly of the genomic region containing genes coding for C-phycocyanin

225   correlated with isolation temperature and measured thermal phenotype. In addition, we measured

226   distinct differences in both thermal resilience of the phycobilisome accessory pigment complex

227   and photosynthetic efficiency (Fv/Fm) between the two thermal ecotypes isolated from different

228   temperatures. These genomic and photophysiological differences are consistent with previous

229   work examining thermal adaptation in marine *Synechococcus*. For instance, it has been suggested

230   that differences in light-harvesting machinery can explain the global distribution of

231   *Synechococcus* clades across large temperature differences (27, 28), and variation in a single

232   amino acid in either the α and β units of R-phycocyanin, an ortholog of C-phycocyanin,

233   correlated with *Synechococcus* thermal adaptation (29). Pittera et al. (2017) also found that at

11

234   elevated temperatures a tropical, low-latitude strain had lower fluorescence of the antenna

235   pigment complex (indicating more efficient photosynthetic energy capture) than a sub-polar

236   strain. This is similar to the trend we observed between warm and cool temperature phenotypes

237   in our study (29). Further supporting the role of phycocyanin in *Synechococcus* thermal

238   adaptation, it has been observed that intracellular concentrations of phycobilisome proteins

239   increase under high temperatures (25). It should also be noted that there could be additional, non-

240   genomic factors such as epigenetic effects not tested for in this study that can increase

241   phenotypic heterogeneity within a population, even at a high degree of relatedness. For instance,

242   epigenetic differences have sometimes been found to be associated with bacterial stress

243   responses (30, 31).

244   Although our experimental setup precludes looking at the relative abundance of each

245   ecotype in the original population, we note that the one isolate collected directly from the

246   environment was the cool temperature ecotype. In an environmental context, the average

247   summertime surface water temperature at our sample site for the period from 1957 to 2019 was

248   20.6 °C, with a maximum of 26.5 °C (Figure 5A). This distribution of temperatures falls below

249   the Topt for both ecotypes, but would likely favor cool temperature isolates. Warm temperature

250   isolates were also collected from 30 °C enrichments, 3.5 °C above the highest measured

251   temperature at this site. Average summer SST at this site has been increasing at a rate of 0.03 °C

252   per year since 1957 (Figure 5A), meaning that the average summertime SST in Narragansett Bay

253   will likely increase to ~23 °C by the end of the century. Assuming a similar distribution of

254   temperatures in the year 2100, there will be periods when SST is above the average Topt of the

255   low temperature ecotype, and conditions will favor the high temperature ecotype (Figure 5B).

256   Any continued trend of rising temperatures beyond 2100 will continue to further expand the

257   niche of the warm temperature ecotype.

258   In addition to this intraspecific diversity likely increasing the resilience of this population

259   to long term warming trends, it is also interesting to consider why adaptations to temperatures

260   exceeding current thermal maxima are maintained in this population. The higher growth rates of

261   cool temperature isolates under typical summer conditions suggest that having the warm

262   temperature phenotype has a fitness cost (when defined purely by growth rates), and in theory

263   selection (considering only growth rates) should remove this phenotype from the population

264   (Innan & Kondrashov, 2010 and references therein). Given the temperature trends at this site, it

265   seems unlikely these are seasonal ecotypes, as the shape of thermal curves suggest that the warm

266   temperature phenotype only has a growth advantage above the maximum daily high temperature

267   observed (26.5 °C).

268   An intriguing explanation for this thermal diversity is that these microbes originated in

269   warmer low latitude waters, and were advected into this relatively cooler region as part of the

270   northerly flow of the nearby Gulf Stream. It has been estimated that microbes entrained in the

271   Gulf Stream may experience a range of temperatures as a result of advection that is larger than

272   changes due to seasonal patterns (33). Although Narragansett Bay is a narrow coastal estuary,

273   wind-driven circulation during summer months facilitates persistent exchange between estuarine

274   waters in the Bay and oceanic waters in Rhode Island Sound (34). This has led to the conjecture

275   that allochthonous inputs of sub-tropical phytoplankton could occur (35, 36), which is supported

276   by the well documented recurring appearance of subtropical fish species in Narragansett Bay

277   during the summer (37).

13

278   These coexisting temperature phenotypes are also interesting in the context of marine

279   *Synechococcus* evolution, as temperature is thought to be a key driver of diversity between

280   clades within this group (8, 27). It is possible that intraspecific microdiversity of thermal

281   phenotypes could have been a contributing mechanism in the diversification of *Synechococcus*

282   into the distinct lineages observed today. When a population consisting of multiple thermotypes

283   encounters a novel thermal environment, one phenotype may be selected over another,

284   potentially leading to genetic divergence and speciation. Further studies will be needed on

285   intraspecific microdiversity at this level, between nearly identical strains, to assess its potential

286   role in the evolution of *Synechococcus* and marine microbes in general.

287   Our findings also have implications for our general understanding of biological responses

288   to rising temperatures. It has been shown that there can be a greater diversity of responses to

289   ocean acidification between ecotypes within phytoplankton taxonomic and functional groups,

290   than between them (Schaum et al. 2013, Hutchins et al. 2013). Our findings show that ecotypes

291   with distinct responses to climate warming can co-occur within a single population. This

292   microdiversity in thermal traits also has been detected in other marine phytoplankton. In a

293   similar study conducted within Narragansett Bay, thermal performance curves of recently

294   isolated strains of the diatom genus *Skeletonema* were compared and showed a similar high

295   degree of intraspecific diversity of thermal traits (39). This study also observed a similar

296   significant difference in thermal maxima (Tmax) across strains, and suggested that variability at

297   such thermal limits plays an important role in both ecological and biogeochemical dynamics.

298   Because of the high degree of genetic similarity between these isolates, amplicon sequencing or

299   metagenomic microbial surveys would not be able to detect this level of functional

300   microdiversity.

14

301   Taking together, the findings of the current study and those of the aforementioned diatom

302   study (39) suggests that this type of fine-scale variation may be widespread among marine

303   microbial taxa. In the case of our estuarine *Synechococcus*, this cryptic thermal microdiversity

304   will likely contribute to this population's ability to continue occupying its picoplanktonic niche

305   even in the face of considerable increases in environmental temperatures. Another important

306   implication is that culture studies using a single isolate or strain from a population may

307   underestimate that population's resilience to warming. A better understanding of the existing

308   functional thermal diversity within populations is needed to correctly model the impact that

309   future elevated temperatures will have on microbial communities, and on the biogeochemical

310   cycles that they regulate.

311   **Methods**

312   *Sampling and Cell Isolation*

313   Surface water at a temperature of 22°C and salinity of 28.48 was collected from the

314   Narragansett Bay Time Series site (latitude 41.47, longitude -71.40) on July 18th, 2017 (36).

315   Collected surface water was pre-filtered using 200μm mesh to remove debris and large grazers.

316   In order to select for multiple temperature phenotypes, we split the collected seawater into 18°,

317   22° (control), 26°, and 30° C temperature treatments. Incubations were performed in triplicate 2L

318   polycarbonate bottles under a 12:12 light dark cycle at 150 μmoles photons / m^2 * sec^{-1}. Cultures

319   were amended with nutrients to match F/40 media (40), and diluted semi-continuously with 0.2

320   um-filtered seawater medium when chlorophyll a fluorescence reached a predetermined

321   threshold to prevent nutrient depletion and avoid cells entering stationary phase.

322   At the time of seawater collection and after 10 days, cells from all temperature treatments

323   that were <1.5 μm in diameter with measurable phycocyanin fluorescence were sorted into 96-

324   well plates containing F/20 media (40) using a BD Influx (San Jose, CA, USA). Wells showing

325   growth over time were transferred into artificial seawater (Sunda, Price, & Morel, 2005), and

326   nutrient concentrations were gradually adjusted to F/2 levels (40). All isolates were maintained at

327   22° C at a light intensity of 150 µmoles photons / $m^2 * sec^{-1}$, with weekly transfers into fresh

328   culture medium.

329   *Thermal Performance Assays*

330   Thermal performance curves were obtained from 11 strains sorted from the initial surface

331   seawater and from the 18 and 30 °C treatments (Table 1). This was done by acclimating aliquots

332   of each culture for two weeks to temperatures between 9° and 33°. Temperatures >33° were

333   added where permissible. This temperature range was chosen because it exceeds that of

334   Narragansett Bay (0.5-24.6 °C, Rynearson, Flickinger, & Fontaine, 2020), and encompasses

335   projected SST increases (20). Strains were grown at each temperature in triplicate 8 ml

336   borosilicate vials containing 5ml of F/2 medium with a 12:12 light:dark cycle and 150 µmoles

337   photons / $m^2 * sec^{-1}$. Biomass was recorded every two days using *in vivo* chlorophyll a

338   fluorescence measured on a Turner AU-10 fluorometer (Turner Designs Inc., Sunnyvale, CA,

339   USA), and growth rates and Eppley-Norberg thermal performance curves (43) were calculated in

340   R (R Team, 2019) using the package growthTools (DOI:10.5281/zenodo.3634918). Cultures

341   containing algal contaminants (verified using fluorescence microscopy) were excluded from the

342   dataset. In two strains, LA20 and LA27, after two weeks of acclimation at 9 °C no

343   *Synechococcus* cells were observed in the culture, so the growth rate was set to zero for these

344   cultures. The thermal performance curve of each strain is hereafter referred to as its phenotype.

345   We verified growth rates for two strains, LA31 and LA127, isolated from low (18 °C)

346   and high (30 °C) temperature treatments respectively using changes in particulate organic carbon

347   (POC). Strains were grown in triplicate in 1L polycarbonate bottles for two weeks at 22 °C

348   (12:12 light:dark cycle and 150 μmoles photons / $m^2 * sec^{-1}$) with dilutions every three days. In

349   addition to POC, carbon fixation was also measured for both strains. Analysis for both POC and

350   carbon fixation were done as in Qu, Fu, & Hutchins (2018) and references therein. At the end of

351   two weeks, cultures were diluted to equal biomass and the temperature was increased to 28 °C.

352   Both isolates were sampled at the beginning, after two days, and after four days.

353   *DNA Extraction, Sequencing, and Analysis*

354   250ml of stationary phase culture for each strain was filtered onto 0.2 μm Polyethersulfone

355   (PES) membrane filters and DNA was extracted using the DNeasy PowerSoil kit (Qiagen,

356   Germantown, MD, USA). Sequencing was done on an Illumina Hiseq, paired-end with 150 base-

357   pair reads (2x150) with ~10 million reads per sample at Novogene Inc. (Beijing, China). The

358   quality of base calls was assessed using fastqc

359   (https://www.bioinformatics.babraham.ac.uk/projects/fastqc), and reads were assembled with

360   SPAdes version 3.13 (46). All programs were run with default settings, unless otherwise noted.

361   To assist in genome curation, reads were assigned taxonomy using Centrifuge version 1.0.4 (47)

362   trained on the "p_compressed+h+v" index (downloaded July 2019), and raw reads were mapped

363   to their assembled genomes using bowtie2 version 2.3.5 (48). The resulting assemblies were

364   curated to remove associated heterotrophs using Anvi'o version 5.5 (49) based on tetranucleotide

365   frequency, coverage, and read taxonomy. Gene calls for curated assemblies were generated using

366   Prodigal version 2.6.3 (50) which were then annotated using kofamScan version 1.1.0 (51) and

367   imported into Anvi'o.

368   In addition to the short-read Illumina sequencing, DNA was extracted from low-

369   temperature (18 °C) strain LA31 and high-temperature (30 °C) strain LA127 for long-read

17

370   sequencing using an Oxford Nanopore Minion (Oxford, UK) with the FLO-MIN106D flow cell.

371   Library prep was done using the Ligation Sequencing Kit (SQK-LSK109) and Rapid Barcoding

372   Kit (SQK-RBK004) following the Genomic DNA by Ligation protocol

373   (https://store.nanoporetech.com/us/media/wysiwyg/pdfs/SQK-

374   LSK109/Genomic_DNA_by_Ligation_SQK-LSK109_-minion.pdf). 200ml of culture grown to

375   stationary phase was concentrated using centrifugation (27,000 x g for 15 minutes) and extracted

376   with the GenElute Bacterial Genomic DNA Kit (Millipore Sigma, Burlington, MA, USA).

377   Basecalling was done using Guppy version 2.2.3 and long reads were filtered using filtLong

378   version 0.2.0 (https://github.com/rrwick/Filtlong). Filtered long reads were mapped to their

379   respective draft assemblies using Minimap2 version 2.17 (52), and the same was done for the

380   short reads using bowtie2 (48). Mapped long and short reads were then assembled together using

381   Unicycler version 0.4.8 (53) with subsequent gene calling and annotation performed as described

382   above.

383   In order to place our isolates in the context of the broader diversity of *Synechococcus,* we

384   pulled all *Synechococcus* genomes (a total of 78 as of July 2019) from NCBI's Refseq (Pruitt &

385   Maglott, 2001; Table S9) and placed them on a phylogenetic tree constructed with GToTree

386   version 1.4.11 (55) using concatenated amino acid sequences for 239 single copy core genes

387   specific to cyanobacteria (using the "Cyanobacteria.hmm" included within GToTree). In short,

388   genes were identified with HMMER3 version 3.2.1 (56), aligned with muscle version 3.8.1551

389   (57), trimmed with trimal 1.4 (58), and concatenated before calculating phylogenetic distance

390   using FastTree2 version 2.1.10 (59). All trees were visualized using the interactive Tree of Life

391   webpage (60). Average nucleotide identity (ANI) was calculated using fastANI version 1.2 (61).

392   The Anvi'o pangenomic pipeline (62) was used to identify gene clusters and to test for gene-

393   cluster correlations with the original incubation temperature from which each strain was isolated.

394   In addition, we looked for sequence variants at loci of interest by mapping reads to the nearest

395   phylogenetic neighbor with a complete genome and profiling single-codon-variants (SCV),

396   utilizing the framework available within Anvi'o (demonstrated at

397   http://merenlab.org/2015/07/20/analyzing-variability/).

398   *Photophysiology Measurements*

399   To analyze differences in photosynthetic accessory pigment function, 200ml of triplicate

400   cultures of low-temperature (18 °C) strain LA31 and high-temperature (30 °C) strain LA127

401   grown to stationary phase at 22 °C were concentrated by centrifuging for 15 minutes at 27,000 x

402   g. Cell pellets were then resuspended in 5ml of sterile media, and the fluorescence and

403   absorption spectra measured on a SpectraMax m2^e (Molecular Devices, San Jose, CA, USA). In

404   order to detect changes in efficiency in the light gathering mechanisms with temperature,

405   fluorescence was measured every three degrees from 22°-57° (10 minute incubation at each

406   temperature) following the methods of Pittera, Partensky, & Six, (2017). This large range of

407   temperatures was used in order to detect the instantaneous disassociation temperature of the

408   phycocyanin antenna complex. Fluorescence emission was measured from 600-700nm (530nm

409   excitation wavelength) matching the profile of the allophycocyanin/phycocyanin pigment

410   complex (63). In addition, we measured the photosynthetic efficiency of photosystem II (Fv/Fm)

411   for these two strains when acclimated to 28° C using a PHYTO-PAM with an excitation

412   wavelength set to 645 nm for C-phycocyanin and allophycocyanin (Heinz Walz, Effeltrich,

413   Germany). Fv/Fm measurements were made using triplicate cultures and three technical

414   replicates each that were dark acclimated for 20 minutes, as in McParland et al. (2019).

415   *Analysis of Long-term Temperature Trends*

416   In order to explore changes in summertime temperature trends at our study site, all

417   available SST data from 1957 through 2019 collected as part of the long-term times series

418   weekly measurements was downloaded from https://web.uri.edu/gso/research/plankton/data/. All

419   measurements from June-August were aggregated by year and a simple linear model (using the

420   lm command in R) used to calculate the rate temperature increase. The slope of this linear model

421   was then used to predict the distribution of summertime temperature in the year 2100. A normal

422   distribution was assumed for both present day and future temperatures, as well as a similar

423   standard deviation from the mean.

424   *Data and Code Availability*

425   Curated genomes are available from SRA under the BioProject ID

426   PRJNA566206. Isolate information and individual BioSample accession numbers can be found

427   in Supplemental Table 2. Scripts used in the analysis and generation of all figures as well as all

428   physiological data are available at https://figshare.com/projects/Kling_et_al_2020/66188.

429   Phenotypic data are also available at: www.bco-dmo.org/award/712792.

430   **Acknowledgements**

20

439 Southern California) and Ben Temperton (University of Exeter) for helping generate and perform

440 base calling on Minion long reads.

References

442 1. J. A. Fuhrman, F. Azam, Thymidine incorporation as a measure of heterotrophic

443 bacterioplankton production in marine surface waters: evaluation and field results. *Mar.*

444 *Biol.* **66**, 109–120 (1982).

445 2. D. G. Capone, *et al.*, Nitrogen fixation by *Trichodesmium spp.*: An important source of

446 new nitrogen to the tropical and subtropical North Atlantic Ocean. *Global Biogeochem.*

447 *Cycles* **19** (2005).

448 3. K. J. Locey, J. T. Lennon, Scaling laws predict global microbial diversity. *Proc. Natl.*

449 *Acad. Sci. U. S. A.* **113**, 5970–5975 (2016).

450 4. M. Chafee, *et al.*, Recurrent patterns of microdiversity in a temperate coastal marine

451 environment. *ISME J.* **12**, 237–252 (2018).

452 5. D. M. Needham, R. Sachdeva, J. A. Fuhrman, Ecological dynamics and co-occurrence

453 among marine phytoplankton, bacteria and myoviruses shows microdiversity matters.

454 *ISME J.* **11**, 1614–1629 (2017).

455 6. T. O. Delmont, *et al.*, Single-amino acid variants reveal evolutionary processes that shape

456 the biogeography of a global SAR11 subclade. *Elife* **8**, 1–27 (2019).

457 7. N. Kashtan, *et al.*, Single-cell genomics reveals hundreds of coexisting subpopulations in

458 wild *Prochlorococcus*. *Science.* **344**, 416–420 (2014).

459 8. J. A. Sohm, *et al.*, Co-occurring *Synechococcus* ecotypes occupy four major oceanic

460 regimes defined by temperature, macronutrients and iron. *ISME J.* **10**, 333 (2016).

461 9. N. García-García, J. Tamames, A. M. Linz, C. Pedrós-Alió, F. Puente-Sánchez,

462   Microdiversity ensures the maintenance of functional microbial communities under

463   changing environmental conditions. *ISME J.* (2019) https:/doi.org/10.1038/s41396-019-

464   0487-8.

465   10.   A. Shade, *et al.*, Fundamentals of microbial community resistance and resilience. *Front.*

466   *Microbiol.* **3**, 417 (2012).

467   11.   M. K. Thomas, C. T. Kremer, C. A. Klausmeier, E. Litchman, A global pattern of thermal

468   adaptation in marine phytoplankton. *Science.* **338**, 1085–1088 (2012).

469   12.   D. A. Hutchins, *et al.*, Climate change microbiology—problems and perspectives. *Nat.*

470   *Rev. Microbiol.* **17**, 391 (2019).

471   13.   R. Cavicchioli, *et al.*, Scientists' warning to humanity: microorganisms and climate

472   change. *Nat. Rev. Microbiol.*, 1 (2019).

473   14.   A. E. Zimmerman, S. D. Allison, A. C. Martiny, Phylogenetic constraints on elemental

474   stoichiometry and resource allocation in heterotrophic marine bacteria. *Environ.*

475   *Microbiol.* **16**, 1398–1410 (2014).

476   15.   D. A. Hutchins, F.-X. Fu, E. A. Webb, N. Walworth, A. Tagliabue, Taxon-specific

477   response of marine nitrogen fixers to elevated carbon dioxide concentrations. *Nat. Geosci.*

478   **6**, 790 (2013).

479   16.   F.-X. Fu, *et al.*, Differing responses of marine N_2 fixers to warming and consequences for

480   future diazotroph community structure. *Aquat. Microb. Ecol.* **72**, 33–46 (2014).

481   17.   N. D. Olson, *et al.*, Metagenomic assembly through the lens of validation: recent advances

482   in assessing and improving the quality of genomes assembled from metagenomes. *Brief.*

483   *Bioinform.*, 1–11 (2017).

484   18.   D. A. Hutchins, F. Fu, Microorganisms and ocean global change. *Nat. Microbiol.* **2**, 17058

485   (2017).

486   19.   J. D. Kling, *et al.*, Transient exposure to novel high temperatures reshapes coastal

487   phytoplankton communities. *ISME J.* (2019) https:/doi.org/10.1038/s41396-019-0525-6.

488   20.   R. K. Pachauri, *et al.*, *Climate change 2014: synthesis report. Contribution of Working*

489   *Groups I, II and III to the fifth assessment report of the Intergovernmental Panel on*

490   *Climate Change* (Ipcc, 2014).

491   21.   M. D. Lee, *et al.*, Marine *Synechococcus* isolates representing globally abundant genomic

492   lineages demonstrate a unique evolutionary path of genome reduction without a decrease

493   in GC content. *Environ. Microbiol.* **21**, 1677–1686 (2019).

494   22.   P. Flombaum, *et al.*, Present and future global distributions of the marine Cyanobacteria

495   *Prochlorococcus* and *Synechococcus*. *Proc. Natl. Acad. Sci. U. S. A*. **110**, 9824–9829

496   (2013).

497   23.   L. Guidi, *et al.*, Plankton networks driving carbon export in the oligotrophic ocean. *Nature*

498   **532**, 465–470 (2016).

499   24.   D. Fucich, D. Marsan, A. Sosa, F. Chen, Complete Genome Sequence of Subcluster 5.2

500   *Synechococcus sp.* Strain CB0101, Isolated from the Chesapeake Bay. *Microbiol. Resour.*

501   *Announc.* **8**, e00484-19 (2019).

502   25.   K. R. M. Mackey, *et al.*, Effect of temperature on photosynthesis and growth in marine

503   *Synechococcus* spp. *Plant Physiol.* **163**, 815–829 (2013).

504   26.   A. W. Thompson, K. Kouba, Differential Activity of Coexisting *Prochlorococcus*

505   Ecotypes. *Front. Mar. Sci.* **6** (2019).

506   27.   J. Pittera, *et al.*, Connecting thermal physiology and latitudinal niche partitioning in

507   marine *Synechococcus*. *ISME J.* **8**, 1221–1236 (2014).

508   28.   T. Grébert, *et al.*, Light color acclimation is a key process in the global ocean distribution

509   of *Synechococcus* cyanobacteria. *Proc. Natl. Acad. Sci. U. S. A.* **115**, E2010–E2019

510   (2018).

511   29.   J. Pittera, F. Partensky, C. Six, Adaptive thermostability of light-harvesting complexes in

512   marine picocyanobacteria. *ISME J.* **11**, 112–124 (2017).

513   30.   L. Hu, *et al.*, Transgenerational epigenetic inheritance under environmental stress by

514   genome-wide DNA methylation profiling in cyanobacterium. *Front. Microbiol.* **9**, 1–11

515   (2018).

516   31.   J. Beaulaurier, *et al.*, Single molecule-level detection and long read-based phasing of

517   epigenetic variations in bacterial methylomes. *Nat. Commun.* **6** (2015).

518   32.   H. Innan, F. Kondrashov, The evolution of gene duplications: Classifying and

519   distinguishing between models. *Nat. Rev. Genet.* **11**, 97–108 (2010).

520   33.   M. A. Doblin, E. Van Sebille, Drift in ocean currents impacts intergenerational microbial

521   exposure to temperature. *Proc. Natl. Acad. Sci. U. S. A.* **113**, 5700–5705 (2016).

522   34.   C. Kincaid, R. A. Pockalny, L. M. Huzzey, Spatial and temporal variability in flow at the

523   mouth of Narragansett Bay. *J. Geophys. Res. C Ocean.* **108**, 11–1 (2003).

524   35.   D. G. Borkman, T. J. Smayda, Gulf Stream position and winter NAO as drivers of long-

525   term variations in the bloom phenology of the diatom *Skeletonema costatum* "species-

526   complex" in Narragansett Bay, RI, USA. *J. Plankton Res.* **31**, 1407–1425 (2009).

527   36.   K. L. Canesi, T. A. Rynearson, Temporal variation of *Skeletonema* community

528   composition from a long-term time series in Narragansett Bay identified using high-

529   throughput DNA sequencing. *Mar. Ecol. Prog. Ser.* **556**, 1–16 (2016).

530   37.   A. J. M. Wood, J. S. Collie, J. A. Hare, A comparison between warm-water fish

531   assemblages of Narragansett Bay and those of Long Island Sound waters. *Fish. Bull.* **107**,

532   89–100 (2009).

533   38.   E. Schaum, B. Rost, A. J. Millar, S. Collins, Variation in plastic responses of a globally

534   distributed picoplankton species to ocean acidification. *Nat. Clim. Chang.* **3**, 298–302

535   (2013).

536   39.   S. I. Anderson, T. A. Rynearson, Variability approaching the thermal limits can drive

537   diatom community dynamics. *Limnol. Oceanogr.*, 1–13 (2020).

538   40.   R. R. L. Guillard, "Culture of phytoplankton for feeding marine invertebrates" in *Culture*

539   *of Marine Invertebrate Animals*, (Springer, 1975), pp. 29–60.

540   41.   W. G. Sunda, N. M. Price, F. M. M. Morel, "Trace metal ion buffers and their use in

541   culture studies" in *Algal Culturing Techniques*, (Elsevier Academic Press London, 2005),

542   pp. 35–63.

543   42.   T. A. Rynearson, S. A. Flickinger, D. N. Fontaine, Metabarcoding Reveals Temporal

544   Patterns of Community Composition and Realized Thermal Niches of *Thalassiosira Spp*.

545   (Bacillariophyceae) from the Narragansett Bay Long - Term Plankton Time Series. **9**, 1–

546   19 (2020).

547   43.   J. Norberg, Biodiversity and ecosystem functioning: A complex adaptive systems

548   approach. *Limnol. Oceanogr.* **49**, 1269–1277 (2004).

549   44.   R. C. Team, R: A language and environment for statistical computing (2019).

550   45.   P. Qu, F. Fu, D. A. Hutchins, Responses of the large centric diatom *Coscinodiscus sp.* to

551   interactions between warming, elevated CO_2, and nitrate availability. *Limnol. Oceanogr.*

552   **63**, 1407–1424 (2018).

553   46.   A. Bankevich, *et al.*, SPAdes: a new genome assembly algorithm and its applications to

554   single-cell sequencing. *J. Comput. Biol.* **19**, 455–477 (2012).

555   47.   D. Kim, L. Song, F. P. Breitwieser, S. L. Salzberg, Centrifuge: rapid and sensitive

556   classification of metagenomic sequences. *Genome Res.* **26**, 1721–1729 (2016).

557   48.   B. Langmead, S. L. Salzberg, Fast gapped-read alignment with Bowtie 2. *Nat. Methods* **9**,

558   357 (2012).

559   49.   A. M. Eren, *et al.*, Anvi'o: an advanced analysis and visualization platform for 'omics

560   data. *PeerJ* **3**, e1319 (2015).

561   50.   D. Hyatt, *et al.*, Prodigal: prokaryotic gene recognition and translation initiation site

562   identification. *BMC Bioinformatics* **11**, 119 (2010).

563   51.   T. Aramaki, *et al.*, KofamKOALA: KEGG ortholog assignment based on profile HMM

564   and adaptive score threshold. *Bioinformatics* **36**, 2251–2252 (2020).

565   52.   H. Li, Minimap2: pairwise alignment for nucleotide sequences. *Bioinformatics* **34**, 3094–

566   3100 (2018).

567   53.   R. R. Wick, L. M. Judd, C. L. Gorrie, K. E. Holt, Unicycler: resolving bacterial genome

568   assemblies from short and long sequencing reads. *PLoS Comput. Biol.* **13**, e1005595

569   (2017).

570   54.   K. D. Pruitt, D. R. Maglott, RefSeq and LocusLink: NCBI gene-centered resources.

571   *Nucleic Acids Res.* **29**, 137–140 (2001).

572   55.   M. D. Lee, GToTree: a user-friendly workflow for phylogenomics. *Bioinformatics*, 1–3

573   (2019).

574   56.   S. R. Eddy, Accelerated profile HMM searches. *PLoS Comput. Biol.* **7** (2011).

575   57.   R. C. Edgar, MUSCLE: multiple sequence alignment with high accuracy and high

576   throughput. *Nucleic Acids Res.* **32**, 1792–1797 (2004).

577   58.   S. Capella-Gutiérrez, J. M. Silla-Martínez, T. Gabaldón, trimAl: a tool for automated

578   alignment trimming in large-scale phylogenetic analyses. *Bioinformatics* **25**, 1972–1973

579   (2009).

580   59.   M. N. Price, P. S. Dehal, A. P. Arkin, FastTree 2–approximately maximum-likelihood

581   trees for large alignments. *PLoS One* **5** (2010).

582   60.   I. Letunic, P. Bork, Interactive Tree Of Life (iTOL): an online tool for phylogenetic tree

583   display and annotation. *Bioinformatics* **23**, 127–128 (2006).

584   61.   C. Jain, L. M. Rodriguez-R, A. M. Phillippy, K. T. Konstantinidis, S. Aluru, High

585   throughput ANI analysis of 90K prokaryotic genomes reveals clear species boundaries.

586   *Nat. Commun.* **9**, 1–8 (2018).

587   62.   T. O. Delmont, A. M. Eren, Linking pangenomes and metagenomes: the *Prochlorococcus*

588   metapangenome. *PeerJ* **6**, e4320 (2018).

589   63.   C. Six, *et al.*, Diversity and evolution of phycobilisomes in marine *Synechococcus spp.*: A

590   comparative genomics study. *Genome Biol.* **8** (2007).

591   64.   E. L. McParland, A. Wright, K. Art, M. He, N. M. Levine, Evidence for contrasting roles

592   of dimethylsulfoniopropionate production in *Emiliania huxleyi* and *Thalassiosira*

593   *oceanica*. *New Phytol.* (2019) https:/doi.org/10.1111/nph.16374.

594

595

27

Figures and Tables
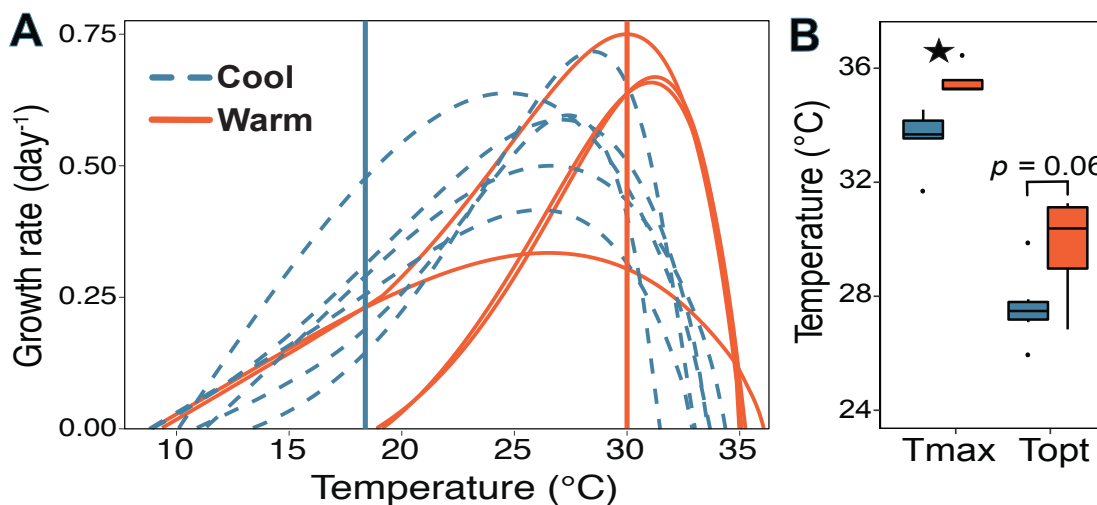
Figure 1: Thermal growth rate responses of *Synechococcus* isolates examined in this study, depending on whether the isolate came from cool (blue; 18-22 °C) or warm (red; 30 °C) incubation experimental temperatu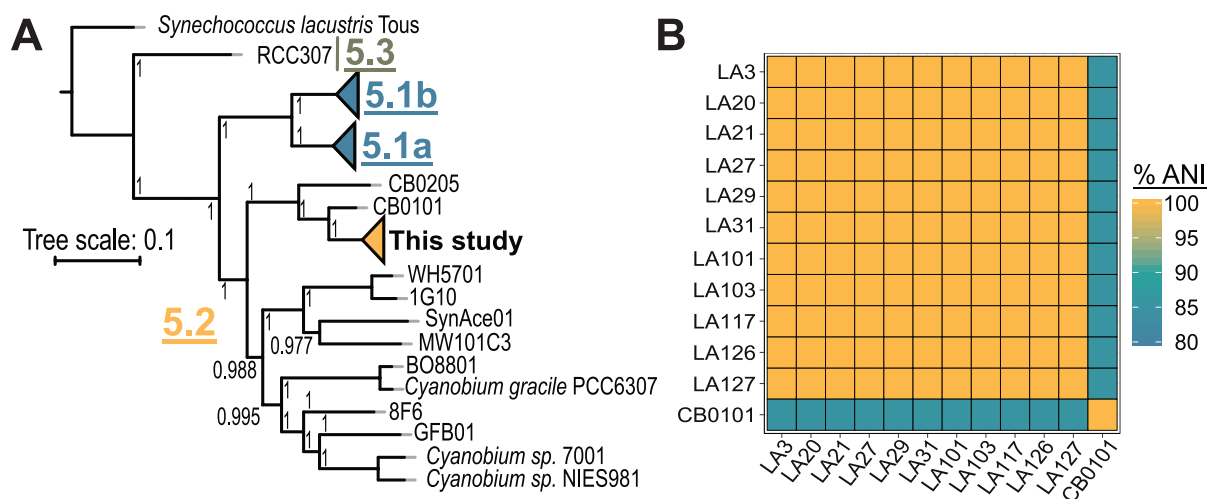res. **A** Thermal Performance Curves (tpc) for all isolates determined using the Eppley-Norberg approach. Vertical lines indicate 18 °C (blue) and 30 °C (red). **B** Boxplots showing the maximum temperature limit (Tmax) and optimal temperature (Topt) for the two sets of isolates. Error bars represent quartiles, and the star indicates $p < 0.05$ level (t-test).

Figure 2: **A** Maximum likelihood tree showing relatedness of the three subclusters (5.1-5.3)

comprising marine *Synechococcus,* using *Synechococcus lacustris* Tous to root the tree.

Phylogenies were established by concatenating AA sequences of 239 single copy core genes.

Scale bar shows AA change per position. **B** Average nucleotide identity (ANI) between all 11

Narragansett Bay isolates from this study. CB0101 from the Chesapeake Bay is the most closely-

related genome present in Genbank and included for comparison.
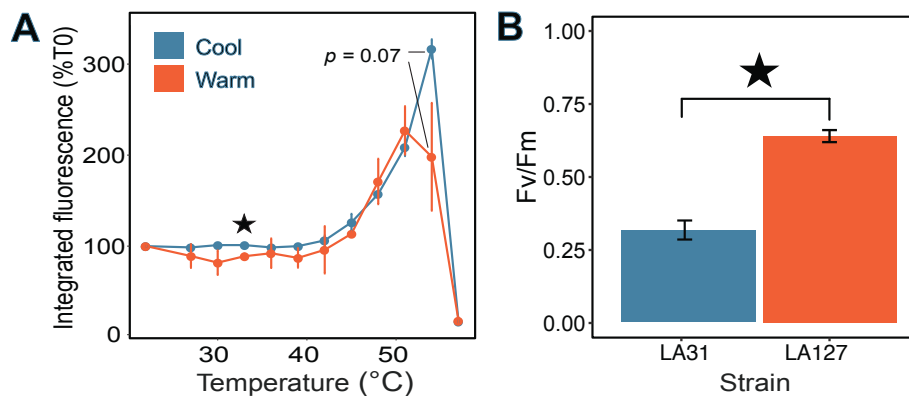
614

615   Figure 3: **A** Mean whole-cell integrated fluorescence (600-700nm) with temperature for warm

616   and cool strains and (**B**) Photochemical efficiency (Fv/Fm) of PSII at an excitation wavelength

617   matching phycocyanin and allophycocyanin (645 nm). Blue colors indicate the cool temperature

618   (18-22 °C) isolate LA31, while red shows warm temperature (30 °C) isolate LA127. The star

619   indicates observations that were statistically different (t-test, $p < 0.05$), and error bars represent ±

620   1 SD from triplicate trials.

621
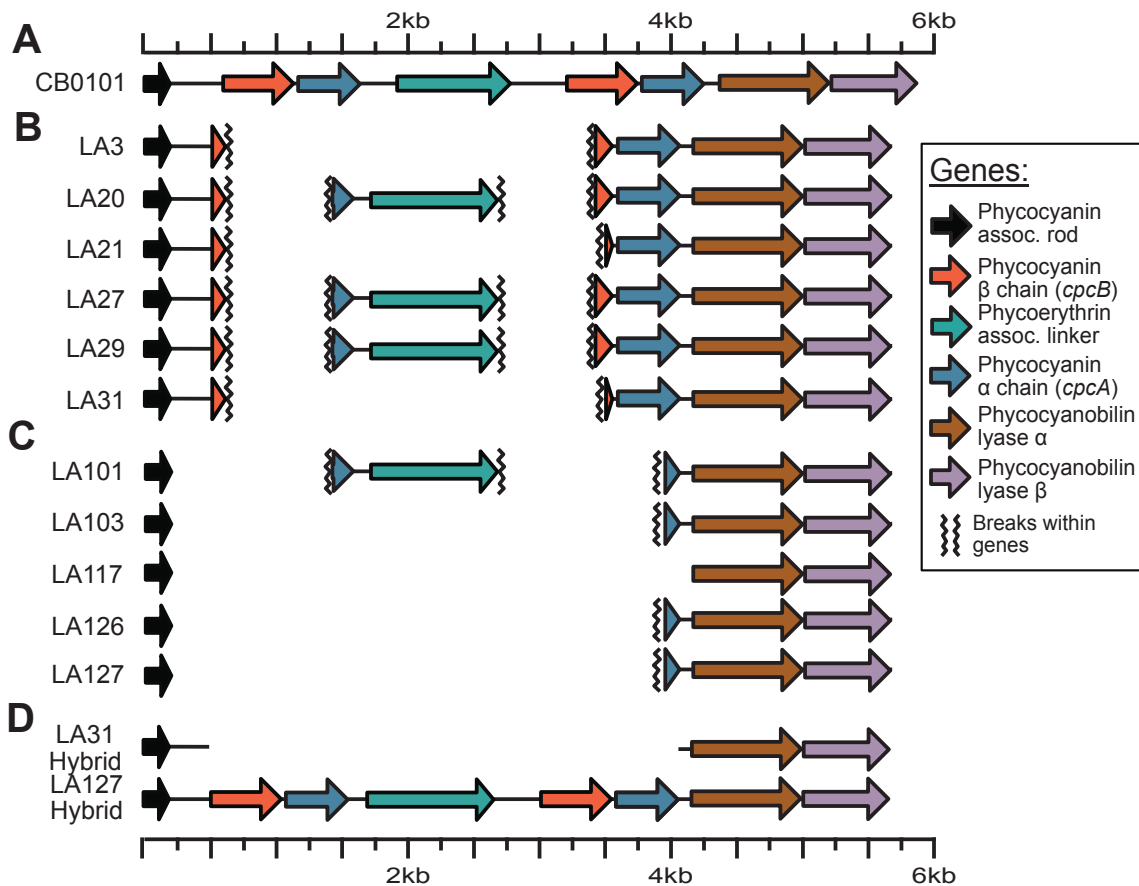
Figure 4: Assembly and coverage information of genes within the locus containing the primary C-phycocyanin genes, *cpcA* (blue arro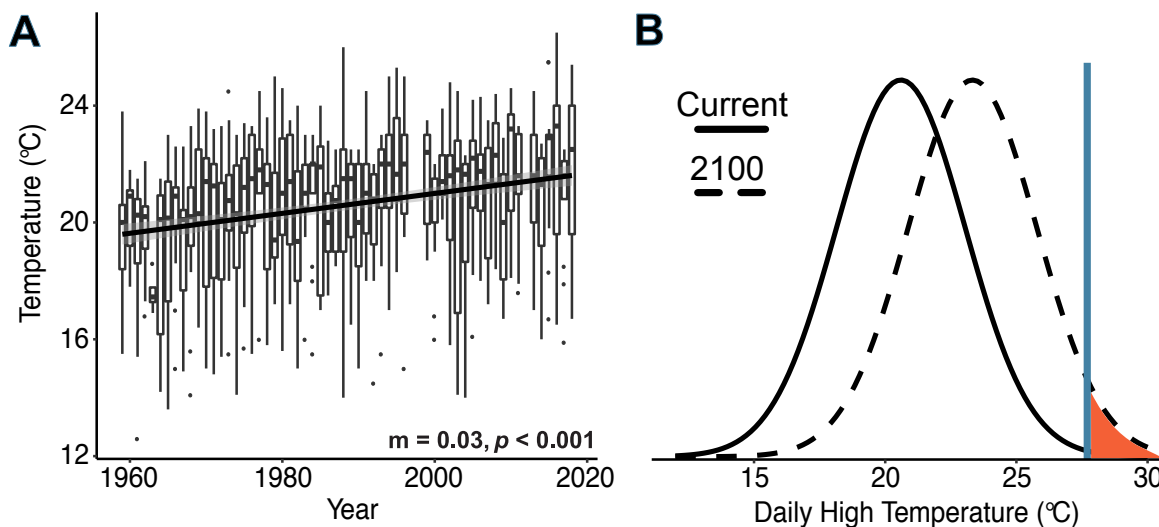ws) and *cpcB* (orange arrows). **A** C-Phycocyanin locus in the closest related genome available on NCBI, CB0101. **B** Structure of draft assemblies of isolates recovered from 18° or 22° **(C)** and 30° C **(D).** Same locus in a cool and warm temperature strain incorporating long reads to close assembly gaps in a hybrid assembly approach.

31

630

631 Figure 5: **A** Boxplot of summertime sea surface temperature (SST) increases at the Narragansett

632 Bay Time Series from 1957 to 2019. Trendline shows the output of a linear model fit to the data.

633 The slope of this model and the *p* value are shown below the data. **B** Hypothetical normal

634 seasonal temperature distributions created using the mean of the recent data shown in panel **A**

635 (solid line), and the predicted distribution of these data in the year 2100 (dashed line) using the

636 slope of the linear model. A blue vertical line shows the average Topt for all cool temperature

637 isolates. Temperatures above this line, which will likely favor warm temperature ecotypes, are

638 shown in red.

639

640 Table 1: Traits derived from thermal performance curves (TPC) characterized for 11

641 *Synechococcus* isolates (indicated with n). TPC parameters are reported in °C.

Temperature	n	Parameter	Mean	SD	Max	Min
22° (Initial)	1	Tmax	33.8			
		Topt	27.9			
		Tmin	11.2			
		Width	21.8			
18°	5	Tmax	33.4	1.0	34.3	31.7
		Topt	27.6	1.4	29.8	26
		Tmin	12.4	3.1	14.8	9.0
		Width	21.0	2.5	24.5	18.9
30°	5	Tmax	35.6	0.5	36.5	35.3
		Topt	29.8	1.8	31.3	26.8
		Tmin	14.2	4.4	19.1	9.0
		Width	21.4	4.7	26.3	16.1

642